Taylor & Francis
Taylor & Francis Group

Numerical Heat Transfer, Part A: Applications
An International Journal of Computation and Methodology

ISSN: 1040-7782 (Print) 1521-0634 (Online) Journal homepage: http://www.tandfonline.com/loi/unht20

Molecular dynamics simulation of water permeation through the Nafion membrane

Zhong-Zhen Li, Lei Chen & Wen-Quan Tao

To cite this article: Zhong-Zhen Li, Lei Chen & Wen-Quan Tao (2016) Molecular dynamics simulation of water permeation through the Nafion membrane, Numerical Heat Transfer, Part A: Applications, 70:11, 1232-1241, DOI: 10.1080/10407782.2016.1230424

To link to this article: https://doi.org/10.1080/10407782.2016.1230424

NUMERICAL HEAT TRANSFER, PART A
2016, VOL. 70, NO. 11, 1232–1241
http://dx.doi.org/10.1080/10407782.2016.1230424

Taylor & Francis
Taylor & Francis Group

Molecular dynamics simulation of water permeation through the Nafion membrane

Zhong-Zhen Li, Lei Chen, and Wen-Quan Tao

Key Laboratory of Thermo-Fluid Science and Engineering, Ministry of Education, School of Energy and Power Engineering, Xi'an Jiaotong University, Xi'an, Shaanxi, People's Republic of China

ABSTRACT

In this paper, the process of water permeation through Nafion membrane is investigated in the atomistic scale. Classic molecular dynamics (MD) simulation is carried out to determine the diffusion of water through the Nafion membrane. Interfacial transport is investigated with non-equilibrium MD simulation. Results indicate that the self-diffusion coefficients increase linearly with water content and agree well with the nuclear magnetic resonance (NMR) experimental results. The interfacial transport coefficients weakly depend on the water contents for high hydration levels and the interfacial resistance can be neglected compared with the diffusion resistance.

ARTICLE HISTORY
Received 22 April 2016
Accepted 9 August 2016

1. Introduction

Polymer electrolyte membrane (PEM) fuel cells are investigated by many investigators during the past decades as a promising type of energy conversion device [1–14]. The permeation of water through the membrane is essential to optimize the operation and design of fuel cells. The permeation of water consists of the transfer across the fluid–membrane interface at the wet side, and the diffusion across the membrane as well as the transfer across the membrane–fluid interface at the dry side. In the past decades, the diffusion of water in the Nafion membrane was studied with molecular dynamics (MD) simulation by many investigators, but the interfacial transport received little attention. Different methods including mass uptake, NMR relaxation, and permeation experiments are used to determine the water transport. But differences in the water diffusivities from those methods vary three orders of magnitude. The dependence of the self-diffusion coefficient on water content is investigated with pulsed field gradient NMR by Zawodzinski et al. [13]. Majsztrik et al. [15] measured the water permeation as a function of water activity and temperature and interfacial mass transport resistance is separated from diffusion resistance by testing different membrane thicknesses.

As a powerful technique in the micro-scale, MD simulations are also used to explore the detailed information about dynamical and structural properties of water molecules in Nafion membrane [16–27]. Jang et al. [22] investigates the effect of monomeric sequence of Nafion chain on their structure and ionic transport. Selvan et al. [23] studied the structural and transport properties of water and hydronium ions at the Nafion–vapor interface and found that the perpendicular component of the vehicular diffusivity of water is large due to the density gradient at the interface where the parallel component is almost the same as the bulk hydrated membrane.

In the present study, equilibrium and non-equilibrium MD simulations are performed to investigate the water diffusion in the bulk hydrated membrane and the interfacial transport at the

CONTACT Wen-Quan Tao wqtao@mail.xjtu.edu.cn Key Laboratory of Thermo-Fluid Science and Engineering, Ministry of Education, Xi'an, Shaanxi 710049, People's Republic of China.
Color versions of one or more of the figures in the article can be found online at www.tandfonline.com/unht.

Nomenclature

a	water activity	***Subscripts***	
j	molar flow rate [mol/cm^2 · s]	m	membrane
k	interfacial transport coefficient [mol/cm^2 · s]	mL	membrane/vapor interface at the wet side
		mg	membrane/vapor interface at the dry side
N	number of molecules	F	Fickian diffusion
s	slope of the graph	g	dry side
λ	water content	i	atom position
		L	wet side
		S	self-diffusion

Nafion–vacuum interface, respectively. The one-dimensional model of water permeation and details about the MD simulations are presented in the next section. In Section 3, the results of the MD simulation and its application for the permeation model are discussed. Finally, some conclusions are drawn in Section 4.

2. Analysis and modeling

2.1. Permeation model

The one-dimensional model of water permeation through Nafion membrane is shown in Figure 1. The membrane is in equilibrium with saturated water vapor at the wet side and in equilibrium with vacuum at the dry side.

The mass transfer rates of water across the interfaces are calculated by Eq. (1) and Eq. (2) for the wet and dry side, respectively.

$$j_{\mathrm{L}} = k_{\mathrm{L}}\ (a_{\mathrm{L}} - a_{\mathrm{mL}}) \tag{1}$$

$$j_{\mathrm{g}} = k_{\mathrm{g}}\ (a_{\mathrm{mg}} - a_{\mathrm{g}}) \tag{2}$$

For simplicity, the transfer resistance at the wet side is neglected here as the water activity a_{L} equals to a_{mL}.

Water diffusion is driven by the water gradient across the membrane and the diffusion rate can be represented by Fick's law as

$$j_{\mathrm{m}} = -D_{\mathrm{F}}\ (\lambda)\ \frac{dC^{\mathrm{m}}}{dz} \tag{3}$$

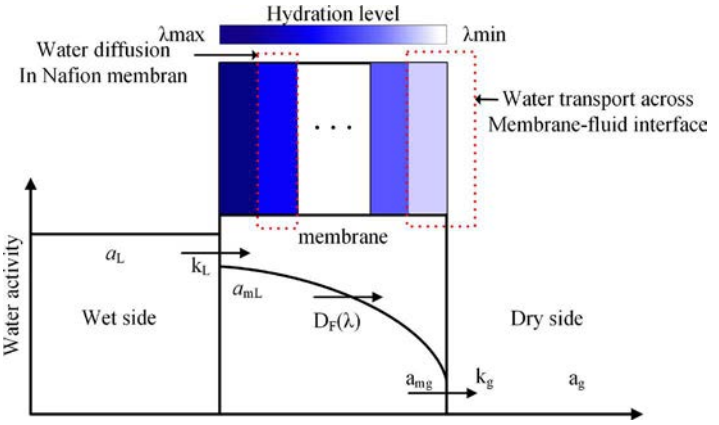

Figure 1. Model of water permeation through the Nafion membrane.

At steady state the permeation rate of water is equal to the mass transfer rate across the membrane–fluid interfaces as well as the water diffusion rate across the membrane.

$$j = j_{\mathrm{L}} = j_{\mathrm{m}} = j_{\mathrm{g}} \tag{4}$$

As illustrated in Eqs. (1)–(4), the diffusion coefficients and mass transfer coefficients are needed to determine the permeation across the membrane. Here, the Nafion membrane is separated as representative volume elements (RVEs) [28] with different water contents in the thickness direction (see Figure 1). With the RVEs, MD simulations are performed to investigate the diffusion coefficients and transport across the interface in the following sections.

2.2. Water diffusion in membrane

Classical MD simulations are performed to investigate the self-diffusion of water in Nafion membrane. As the diffusion coefficients of water are not independent of the water content in the Nafion membrane, 7 cells with different water contents λ (water molecules per SO_3 group) of 2, 4, 6, 8, 10, 12, and 14 are investigated, respectively, through MD simulation.

The initial structure of Nafion membrane containing nine polymer chains is constructed with Amorphous Cells modules of Materials Studio 6.1 from Accelrys Software Inc. The molecular structure of each polymer chain consisting 682 atoms is shown in Figure 2. After the Nafion membrane structure is obtained in cells, 90 H_3O^+ molecules are added to make the system electrically neutral and 180–1,260 water molecules are added for different water contents with GROMACS 4.5.4 [29]. Then energy minimization with a steepest descent algorithm is performed for simulation cells to obtain a stable configuration.

After minimization of energy for each cell, the structure is relaxed by applying multiple annealing processes between 300 and 600 K. Each annealing procedure is followed by a 10 ns NPT MD at 0.1 MPa to fully equilibrate the structures at different target temperatures (300 and 340 K). For each equilibrium structure, production simulation run containing 20 ns NVT MD simulation is performed and the configurations are saved every 1 ps for subsequent analysis of structural and dynamics properties.

GROMACS 4.5.4 [29] is used to perform the MD simulations. The DREIDING force field [30] including recent modifications to the fluorocarbon part by other investigators [31] is used to describe inter- and intramolecular interactions of polymer chains of Nafion, and the flexible three-center (F3C) force field [32] is used for water and H_3O^+.

With the results of classical MD simulations, the structural and thermodynamics properties, such as the density and diffusion coefficient, can be extracted. The self-diffusion coefficients of water molecules in Nafion can be estimated by studying its mean square displacement (MSD):

$$\mathrm{MSD}(t) = \frac{1}{N}\left\langle \sum_{i=1}^{N_{\mathrm{m}}} [\vec{r}_i(t) - \vec{r}_i(0)]^2 \right\rangle \tag{5}$$

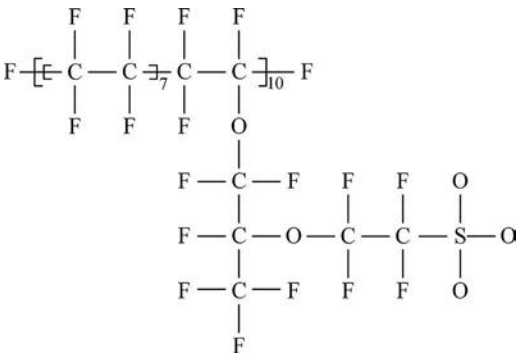

Figure 2. Molecular structure of a polymer chain of the Nafion membrane.

where $\vec{r}_i(t)$ and $\vec{r}_i(0)$ denote the location of particle i at time t and the initial location, respectively. N is the number of particles in system and the angular brackets denote an ensemble average of system. For large time separation, the MSD scales linearly as t. So according to the Einstein expression:

$$D_S = \lim_{t\to\infty} \frac{1}{6Nt} \left\langle \sum_{i=1}^{N_m} [\vec{r}_i(t) - \vec{r}_i(0)]^2 \right\rangle \tag{6}$$

The self-diffusion coefficients can be calculated as:

$$D_S = \lim_{t\to\infty} \frac{\mathrm{MSD}(t)}{6t} = \frac{s}{6} \tag{7}$$

where s represents the slope of the MSD linear fitting with t.

In the present study, the diffusion of water molecules with water concentration gradient is described by Fick's law (see Eq. (3)). The relation between the Fickian and self- diffusion coefficients can be represented as [33]:

$$D_F = D_S \left[\frac{\partial \ln(a)}{\partial \ln(\lambda)}\right] \tag{8}$$

where a represents the water activity, and its relationship with water content λ used in the present study is given by

$$\lambda = 0.043 + 17.81a - 39.85a^2 + 36.0a^3 \tag{9}$$

Eq. (9) represents the water content of a Nafion membrane in contact with water vapor measured at 303.15 K by Zawodzinski et al. [3]; it is assumed to be valid at other temperatures [12]. The water content varies from 0.043 to 14 as the water activity changes from 0 to 1 according to Eq. (9).

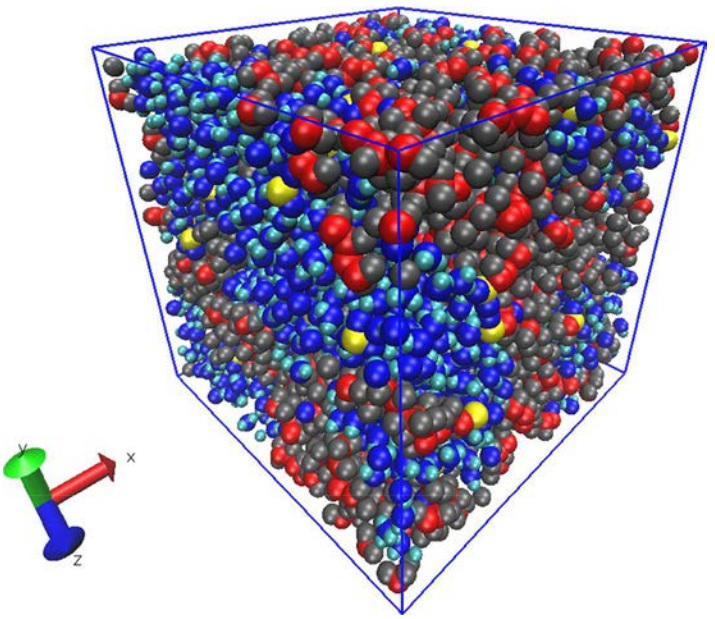

Figure 3. Snapshot of the simulation box of the Nafion membrane with water content $\lambda = 14$: red, C; gray, F; yellow, S; blue, O; cyan, H.

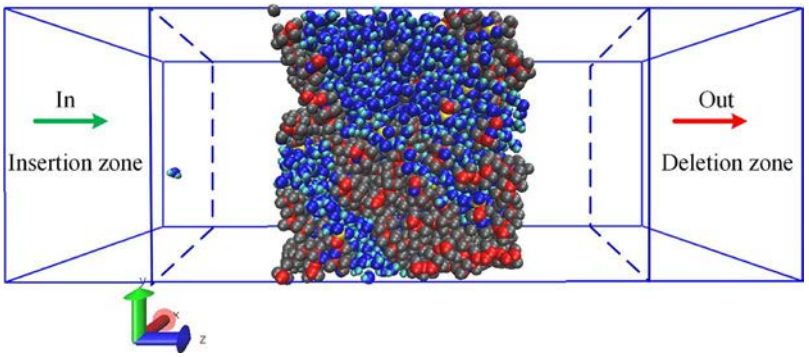

Figure 4. Snapshot of the non-equilibrium MD simulation of water transport across the membrane–vapor interface.

2.3. Water transport across the membrane–vapor interface

Non-equilibrium MD simulations are performed to investigate the water transport across the membrane–vapor interface. As shown in Figure 4, the simulation model is a box with an RVE in the middle of the z-axis. In this section, RVEs with water contents λ of 2, 4, 6, 8, 10, 12, and 14 at 300 and 340 K are investigated, respectively. The length in z-direction is 150 Å and the dimension in x–y plane is different for RVE with different water contents. The periodic boundary condition is applied for x and y directions, and the boundaries in z-directions are treated as fixed walls.

The large-scale atomic/molecular massively parallel simulation (LAMMPS) [34] with the force field described in the previous section is used on a computing cluster system. To model the membrane equilibrium with vacuum at the dry side, as shown in Figure 4, a deletion zone between 140 and 150 Å in z-direction of the simulation box is defined where water molecules are removed. In order to model a steady-state transfer process, an insertion zone between 0 and 10 Å is defined where the same number of water molecules are inserted once removed in deletion zone. The water transfer rate j, defined as the number of water molecules removed or inserted per unit time and area, is calculated as

$$j = \frac{\mathrm{d}N_{\mathrm{W}}}{A\mathrm{d}t} \tag{10}$$

where N_{W} represents the total number of water molecules removed in the deletion zone and A denotes the area of x–y plane in the simulation box. Before the transfer process is initiated, the system is in equilibrium with its vapor for a 10 ns simulation.

3. Results and discussion

3.1. Diffusion

Figure 5 shows the MSD of water molecules in Nafion with water content from 2 to 14 at temperature of 300 K. The MSD of water molecules scales linearly as the simulation time t and the slope increases with hydration level. With the MSD of water molecules, self-diffusion coefficients can be calculated with Eq. (7) for different hydration levels and compared with the pulsed gradient NMR experiment [13] (see Figure 6). The results of MD simulations at 300 K are agreed well with the experiment at 303.15 K and the diffusion coefficients of MD simulation at 340 K are larger than that at 300 K for the same hydration level. The diffusion coefficients increase linearly with hydration levels and here we fit these values to linear expressions in Eq. (11) and Eq. (12) for 300 and 340 K, respectively.

$$D_{\mathrm{S}} = (-0.899 + 0.52\lambda) \times 10^{-6} \tag{11}$$

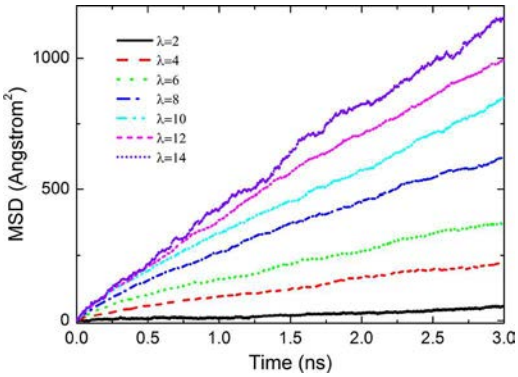

Figure 5. MSD of water molecules in Nafion at different hydration levels.

$$D_S = (-1.328 + 1.023\lambda) \times 10^{-6} \tag{12}$$

Note that Eq. (11) and Eq. (12) are applied with λ ranging from 2 to 14. For $0 < \lambda < 2$, D_S is assumed to linearly increase from 0 to $D_S(\lambda = 2)$. With D_S from Eq. (11) and Eq. (12), the Fickian diffusion coefficients D_F can be obtained with Eq. (8) and Eq. (9) (see Figure 7).

3.2. Interfacial transport coefficient

With the water density profile across the transfer direction, the water transport characteristics can be obtained and determined whether the water transport reaches steady state or not. In Figure 8, water density profiles of Nafion for different hydration levels and temperatures are shown. When the membrane is in equilibrium with water vapor after a 10 ns simulation, the water density near the interface decreases to a vapor density due to the dehydration of membrane contact with vapor. The water density increases in the half of membrane near the deletion zone, whereas decreases in the other half due to the migration of water molecules along the z-direction during the water transfer. Figure 9 shows the N_W for different λ and temperature during the transfer.

The N_W increases linearly with time and the transfer rate j can be estimated with Eq. (10) by linear fitting the N_W with time. Table 1 shows the transfer rate j for different hydration levels at different temperatures.

The interfacial transport coefficients can be estimated with the transfer rate j by Eq. (2). Note that the water activity in membrane a_{mg} is estimated by Eq. (9). The vapor activity a_g is zero for water

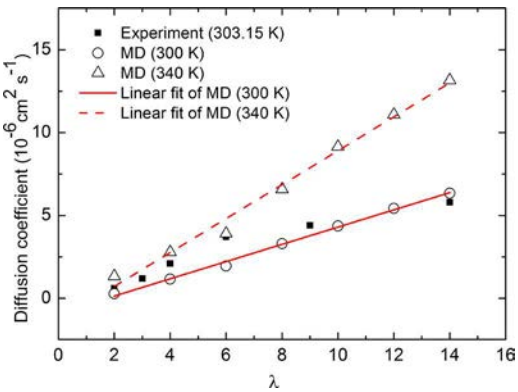

Figure 6. Diffusion coefficients of water molecules at different water hydration levels from the present MD simulation and experiment.

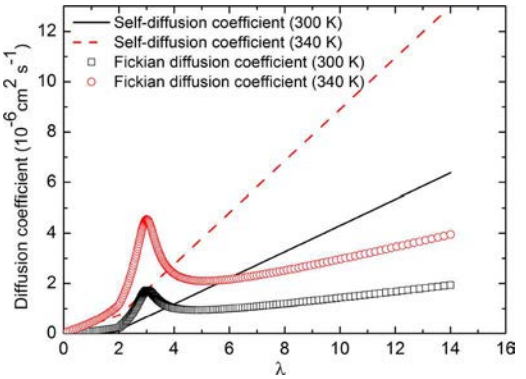

Figure 7. Self- and Fickian diffusion coefficients in Nafion at different hydration levels.

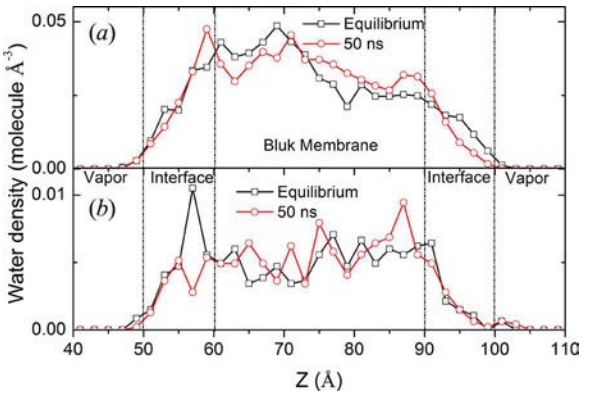

Figure 8. Water density profile across the permeation direction: (a) $\lambda = 14$, $T = 340$ K; (b) $\lambda = 2$, $T = 300$ K. The short dash-dot line represents the membrane–vapor interface.

transfer into vacuum. Figure 10 shows the interfacial transport coefficients for different water contents at different temperatures.

The interfacial transport coefficients at 340 K are an order of magnitude larger than that at 300 K and the transport coefficients weakly depend on the water contents for high hydration levels. The

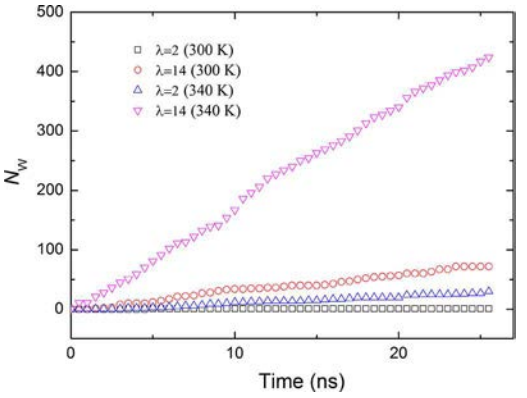

Figure 9. The total number of water molecules removed in the deletion zone.

Table 1. Transfer rate for different water contents and temperatures.

Water content	Temperature (K)	Transfer rate (mol/cm^2 · s)
2	300	6.72E −04
	340	8.45E −03
4	300	4.48E −03
	340	2.25E −02
6	300	8.06E −03
	340	5.49E −02
8	300	1.06E −02
	340	6.70E − 02
10	300	1.09E −02
	340	9.21E −02
12	300	1.37E −02
	340	7.28E −02
14	300	1.31E −02
	340	1.02E −01

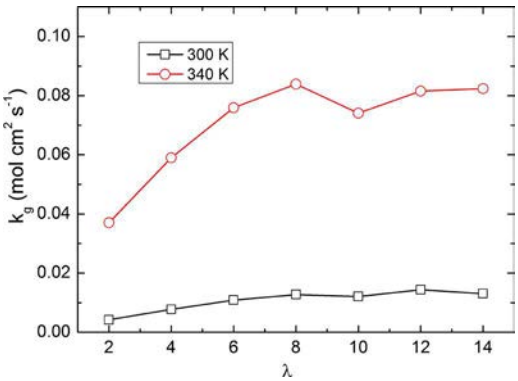

Figure 10. The interfacial transport coefficients for different water contents at different temperatures.

interfacial transport coefficients are extraordinarily larger than the results from the experiment [15]. It is because in the permeation experiment, an N_2 flow is maintained on the dry side of membrane and a gas phase boundary layer and Teflon-like surface is formed at the vapor–membrane interface [10], which takes the main contribution of interfacial resistance. Whereas for our non-equilibrium MD simulation, the interfacial resistance decreases rapidly without the gas phase boundary layer, and the Teflon-like surface as the membrane is in contact with vacuum.

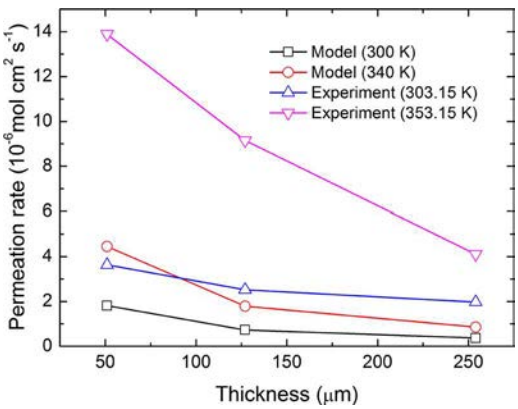

Figure 11. The permeation rate for water activity $a_L = 0.8$ and $a_g = 0.2$.

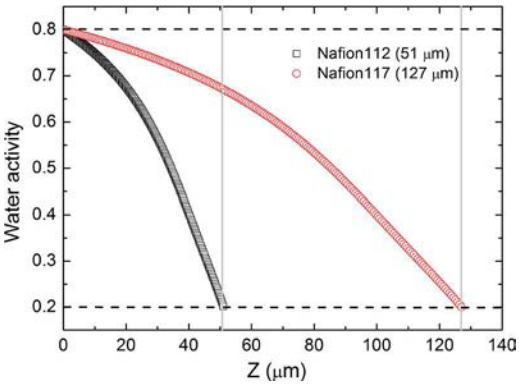

Figure 12. Water activity profile across the Nafion membrane with different thicknesses.

3.3. Permeation rate

With the Fickian diffusion coefficient and interfacial transport coefficient obtained in the previous sections, the permeation rate can be estimated by Eqs. (1)–(4) for given water activities in the two sides of membrane. The predicted permeation rates through Nafion membranes are compared with the experimental rates [15] in Figure 11.

Figure 12 shows the water activity distribution across the membrane predicted by model with the water activity $a_L = 0.8$ and $a_g = 0.2$. We can see that the water activity in the membrane near the dry side (a_{mg}) is almost equal to 0.2. That means the interfacial resistance can be neglected compared with the diffusion resistance. In other words, the permeation is limited by water diffusion and the permeation rates scale inversely with membrane thickness, as shown in Figure 11.

4. Conclusions

Water permeation through the Nafion membrane is controlled by the characteristics of water diffusivity and interfacial mass transport. These characteristics of water are investigated separately by MD simulations.

The predicted self-diffusion coefficients increase linearly with water content and agree well with the NMR experimental results. The interfacial transport coefficients at 340 K are an order of magnitude larger than that at 300 K. The interfacial transport coefficients weakly depend on the water contents for high hydration levels, and the interfacial resistance can be neglected compared with the diffusion resistance. The permeation is limited by water diffusion in membrane as the membrane is in contact with vapor water.

Funding

This work has been supported by the National Natural Science Foundation of China (grant number 51136004) and the 111 Project (B16038).

References

[1] T. E. Springer, T. A. Zawodzinski, and S. Gottesfeld, Polymer Electrolyte Fuel Cell Model, *J. Electrochem. Soc.*, vol. 138, no. 8, pp. 2334–2342, 1991.
[2] A. Z. Weber and J. Newman, Transport in Polymer-Electrolyte Membranes: I. Physical Model, *J. Electrochem. Soc.*, vol. 150, no. 7, pp. A1008–A1015, 2003.
[3] T. A. Zawodzinski et al., A Comparative Study of Water Uptake by and Transport Through Ionomeric Fuel Cell Membranes, *J. Electrochem. Soc.*, vol. 140, no. 7, pp. 1981–1985, 1993.
[4] L. Chen, et al., Numerical Investigation of Liquid Water Distribution in the Cathode Side of Proton Exchange Membrane Fuel Cell and its Effects on Cell Performance, *Int. J. Hydrogen Energy*, vol. 37, no. 11, pp. 9155–9170, 2012.

[5] L. Chen, et al., Multi-scale Modeling of Proton Exchange Membrane Fuel Cell by Coupling Finite Volume Method and Lattice Boltzmann Method, *Int. J. Heat Mass Transfer*, vol. 63, pp. 268–283, 2013.
[6] L. Chen, Y.-L. He, and W.-Q. Tao, Effects of Surface Microstructures of Gas Diffusion Layer on Water Droplet Dynamic Behaviors in a Micro Gas Channel of Proton Exchange Membrane Fuel Cells, *Int. J. Heat Mass Transfer*, vol. 60, pp. 252–262, 2013.
[7] L. Chen, et al., Pore-Scale Flow and Mass Transport in Gas Diffusion Layer of Proton Exchange Membrane Fuel Cell with Interdigitated Flow Fields, *Int. J. Therm. Sci*., vol. 51, pp. 132–144, 2012.
[8] S. Ge, et al., Absorption, Desorption, and Transport of Water in Polymer Electrolyte Membranes for Fuel Cells, *J. Electrochem. Soc*., vol. 152, no. 6, pp. A1149–A1157, 2005.
[9] K. Jiao and X. Li, Water Transport in Polymer Electrolyte Membrane Fuel Cells, *Prog. Energy Combust. Sci*., vol. 37, no. 3, pp. 221–291, 2011.
[10] P. W. Majsztrik, et al., Water Sorption, Desorption and Transport in Nafion Membranes, *J. Membr. Sci*., vol. 301, no. 1–2, pp. 93–106, 2007.
[11] D. R. Morris and X. Sun, Water-Sorption and Transport Properties of Nafion 117 H, *J. Appl. Polym. Sci*., vol. 50, no. 8, pp. 1445–1452, 1993.
[12] S. Motupally, A. J. Becker, and J. W. Weidner, Diffusion of Water in Nafion 115 Membranes, *J. Electrochem. Soc*., vol. 147, no. 9, pp. 3171–3177, 2000.
[13] T. A. Zawodzinski, et al., Determination of Water Diffusion Coefficients in Perfluorosulfonate Ionomeric Membranes, *J. Phys. Chem*., vol. 95, no. 15, pp. 6040–6044, 1991.
[14] Q. Zhao, P. Majsztrik, and J. Benziger, Diffusion and Interfacial Transport of Water in Nafion, *J. Phys. Chem. B*, vol. 115, no. 12, pp. 2717–2727, 2011.
[15] P. Majsztrik, A. Bocarsly, and J. Benziger, Water Permeation Through Nafion Membranes: The Role of Water Activity, *J. Phys. Chem. B*, vol. 112, no. 51, pp. 16280–16289, 2008.
[16] A. Elliott, J., Atomistic Simulation and Molecular Dynamics of Model Systems for Perfluorinated Ionomer Membranes, *Phys. Chem. Chem. Phys*., vol. 1, no. 20, pp. 4855–4863, 1999.
[17] L. Chen, Y.-L. He, and W.-Q. Tao, The Temperature Effect on the Diffusion Processes of Water and Proton in the Proton Exchange Membrane Using Molecular Dynamics Simulation, *Numer. Heat Transfer, Part A*, vol. 65, no. 3, pp. 216–228, 2013.
[18] S. Cui, et al., A Molecular Dynamics Study of a Nafion Polyelectrolyte Membrane and the Aqueous Phase Structure for Proton Transport, *J. Phys. Chem. B*, vol. 111, no. 9, pp. 2208–2218, 2007.
[19] K. B. Daly, et al., Molecular Dynamics Simulations of Water Sorption in a Perfluorosulfonic Acid Membrane, *J. Phys. Chem. B*, vol. 117, no. 41, pp. 12649–12660, 2013.
[20] R. Devanathan, and A. Venkatnathan, and M. Dupuis, Atomistic Simulation of Nafion Membrane: I. Effect of Hydration on Membrane Nanostructure, *J. Phys. Chem. B*, vol. 111, no. 28, pp. 8069–8079, 2007.
[21] R. Devanathan, A. Venkatnathan, and M. Dupuis, Atomistic Simulation of Nafion Membrane. 2. Dynamics of Water Molecules and Hydronium Ions, *J. Phys. Chem. B*, vol. 111, no. 45, pp. 13006–13013, 2007.
[22] S. S. Jang, et al., Nanophase-Segregation and Transport in Nafion 117 from Molecular Dynamics Simulations: Effect of Monomeric Sequence, *J. Phys. Chem. B*, vol. 108, no. 10, pp. 3149–3157, 2004.
[23] M. E. Selvan, et al., Molecular Dynamics Study of Structure and Transport of Water and Hydronium Ions at the Membrane/Vapor Interface of Nafion, *J. Phys. Chem. C*, vol. 112, no. 6, pp. 1975–1984, 2008.
[24] Y.-L. S. Tse, et al., Molecular Dynamics Simulations of Proton Transport in 3 M and Nafion Perfluorosulfonic Acid Membranes, *J. Phys. Chem. C*, vol. 117, no. 16, pp. 8079–8091, 2013.
[25] S. Urata, et al., Molecular Dynamics Simulation of Swollen Membrane of Perfluorinated Ionomer, *J. Phys. Chem. B*, vol. 109, no. 9, pp. 4269–4278, 2005.
[26] A. Vishnyakov and A. V. Neimark, Molecular Simulation Study of Nafion Membrane Solvation in Water and Methanol, *J. Phys. Chem. B*, vol. 104, no. 18, pp. 4471–4478, 2000.
[27] A. Vishnyakov and A. V. Neimark, Molecular Dynamics Simulation of Microstructure and Molecular Mobilities in Swollen Nafion Membranes, *J. Phys. Chem. B*, vol. 105, no. 39, pp. 9586–9594, 2001.
[28] M. Ozmaian and R. Naghdabadi, Modeling and Simulation of the Water Gradient within a Nafion Membrane, *Phys. Chem. Chem. Phys*., vol. 16, no. 7, pp. 3173–3186, 2014.
[29] S. Pronk, et al., GROMACS 4.5: A High-Throughput and Highly Parallel Open Source Molecular Simulation Toolkit, *Bioinformatics*, vol. 29, no. 7, pp. 845–854, 2013.
[30] S. L. Mayo, B. D. Olafson, and W. A. Goddard, Dreiding - a Generic Force-Field for Molecular Simulations, *J. Phys. Chem*., vol. 94, no. 26, pp. 8897–8909, 1990.
[31] S. S. Jang, et al., The Source of Helicity in Perfluorinated N-alkanes, *Macromolecules*, vol. 36, no. 14, pp. 5331–5341, 2003.
[32] M. Levitt, et al., Calibration and Testing of a Water Model for Simulation of the Molecular Dynamics of Proteins and Nucleic Acids in Solution, *J. Phys. Chem. B*, vol. 101, no. 25, pp. 5051–5061, 1997.
[33] W. Weppner and R. A. Huggins, Determination of Kinetic-Parameters of Mixed-Conducting Electrodes and Application to System Li3sb, *J. Electrochem. Soc*., vol. 124, no. 10, pp. 1569–1578, 1977.
[34] S. Plimpton, Fast Parallel Algorithms for Short-range Molecular Dynamics, *J. Comput. Phys*., vol. 117, no. 1, pp. 1–19, 1995.